

Article

A Study on the Development and Evolution of Fractures in the Coal Pillar Dams of Underground Reservoirs in Coal Mines and Their Optimum Size

Bao Zhang ^{1,2,*}, Wei Ni ², Xiuqiang Hao ², Huiqiang Li ² and Yupeng Shen ^{1,*}

¹ School of Energy and Mining Engineering, China University of Mining and Technology-Beijing, Beijing 100083, China

² CHN Energy Technology & Economics Research Institute, Beijing 102211, China

* Correspondence: 13716180380@163.com (B.Z.); cumtbsyp@163.com (Y.S.)

Abstract: The western mining areas of China, which are rich in coal resources, lack water resources. Large-scale and high-intensity coal mining in China's western mining areas has led to the loss of groundwater resources. Underground reservoirs in coal mines are an effective means of achieving the protection and utilization of water resources in these western mining areas. One of the important standards for the safety of an underground reservoir in a coal mine involves checking whether the development of cracks in the coal pillar dam body, under the dual stress conditions of overlying strata and lateral water pressure, passes through the coal pillar dam body or its top and bottom plates, forming a seepage channel for mine water. This article focuses on the safety issues associated with coal pillar dams in the underground reservoirs of coal mines. From the perspectives of overlying rock pressure and lateral water pressure on coal pillar dams, mechanical models, numerical calculations, and similar simulation methods were used to analyze macroscopic deformation, displacement, and crack development in coal pillar dams of different sizes under vertical and horizontal stress and to study the optimum width of coal pillar dams. Our research results indicated that the optimal width of the coal pillar dam body can be determined via numerical simulation based on the deformation and stress state in a given dam. When the horizontal stress increases, the smaller the coal pillar width is, the greater the increment of s_{yy} and s_{xx} becomes, and the more likely the coal pillar is to be damaged. Similar simulations showed that the smaller the size of the coal pillar is, the easier it is to generate stress concentration, and the more likely this stress is to "eat away" the coal pillar dam body. There is a certain relationship between the size of the coal pillar dam and the range of crack development. The larger the coal pillar size is, the less obvious the stress concentration effect becomes, and the less likely the crack is to penetrate the internal and external parts of the reservoir. Taking the Shangwan mine as an example, it was determined that the maximum water head height that could be carried by the 15-m coal pillar dam body was 50 m. A comprehensive study of the development and evolution of cracks in the coal pillar dam of an underground reservoir in a coal mine, and the characteristics of sliding instability, was conducted to determine the optimal size and maximum water storage height of a coal pillar that does not penetrate the inner and outer parts of the reservoir. The development and evolution of cracks are important factors affecting the stability of coal pillar dams. This study can expand and improve the basic theory of underground reservoirs in coal mines, provide a scientific basis for determining the optimum size of a coal pillar dam, guarantee the long-term safe and stable operation of the coal pillar dams of underground reservoirs in coal mines, and continuously save mine water resources and increase the economic benefits of coal mines. These implications are of great significance for the long-term stable operation of underground reservoirs in coal mines under similar geological conditions.

Keywords: coal mine underground reservoir; coal pillar dam; fissure development and evolution law; optimum size of coal pillar; maximum water level



Citation: Zhang, B.; Ni, W.; Hao, X.; Li, H.; Shen, Y. A Study on the Development and Evolution of Fractures in the Coal Pillar Dams of Underground Reservoirs in Coal Mines and Their Optimum Size. *Processes* **2023**, *11*, 1677. <https://doi.org/10.3390/pr11061677>

Academic Editor: Ján Pitel'

Received: 5 April 2023

Revised: 21 May 2023

Accepted: 26 May 2023

Published: 31 May 2023



Copyright: © 2023 by the authors. Licensee MDPI, Basel, Switzerland. This article is an open access article distributed under the terms and conditions of the Creative Commons Attribution (CC BY) license (<https://creativecommons.org/licenses/by/4.0/>).

1. Introduction

Coal currently has the most stable energy supply and the highest independent guaranteed supply rate, and is the most economic basic energy, in China, and has always guaranteed the energy security of China [1–3]. The overall distribution pattern of coal resources in China is “more in the north and less in the south, more in the west and less in the east, deep in the east and dry in the west” [4,5]. Following years of high-intensity mining, the coal resources in the east and central regions have tended to be exhausted, and coal production has been transferred to the western provinces, which contributed 81% of China’s coal production in 2022. However, the water resources in the western mining area are extremely short, accounting for only 3.9% of the country’s water resources, and the ecological environment in the western area is fragile. According to the relevant statistics, every 1 ton of coal mined in China produces approximately 2 tons of mine water; however, to date, the rate of mine water utilization has only been approximately 25% [6]. Most of the produced mine water is discharged to the ground, not only causing the waste of water resources due to evaporation but also polluting the environment [7,8]. The Shendong mining area is the world’s only 200-million-ton mining area, with seven mines producing an annual output of more than 10 million tons. The Shendong mining area is located on the edge of the arid and water-scarce Maowusu Desert, where the ecological environment is extremely fragile and water resources are extremely scarce [9]. Coal mining causes the destruction of water resources, accelerates the loss of surface water, and leads to more and more prominent problems of water use in mining areas. After years of exploration and practice, more than 30 underground reservoirs of coal mines have been successfully built in the Shendong Mining area, and this has largely solved the problem of water resource protection and utilization in the mining area and protected the area’s ecological environment. With the continuous popularization and application of underground reservoir technology in coal mines, more and more attention has been paid to the long-term operational safety of underground reservoirs in coal mines—especially the safety of coal pillar dams—and this has become key to ensuring the long-term safe operation of underground reservoirs in coal mines.

Based on the 20 years of technical exploration and engineering practice in the Shendong mining area, academician Gu Dazhao [10] put forward the theoretical framework and technical system of underground reservoirs for coal mines with “transport, storage and use” as the core themes. The idea of using the goaf as an underground water storage space was thus conceived, creating a new way to protect and utilize mine water resources in the process of coal mining. A large number of engineering practices have since been carried out and good results have been achieved [11,12]. Based on theoretical analysis and numerical simulation, Pang Yihui [13] comprehensively analyzed the feasibility of building an underground reservoir in a coal mine under the condition of large mining height. In their study of coal mining stress fields, B. Unver and Zhang Guojun [14,15] established a three-dimensional calculation model to analyze the movement law of overlying strata and its mining response mechanism in thick coal seam mining. Rajendra Singh [16] studied the variation law of mining stress and the movement law of overlying strata in thick coal seam mining through field testing. Zhang Nong [17] analyzed the failure characteristics and the stability of roof roadways in relief mining. Kong Xiangsong and Shan Renliang [18] established the theoretical expression of stress waves and the dynamic constitutive model of coal, and studied the classification of surrounding rock and the theory of dynamic pressure resistance. In a study on coal pillar dams, Ashok Jaiswal and B.K. Shrivastva [19] established a numerical calculation model and used the strain softening constitutive model to study the strengths of coal pillars. Robert Bertuzzi et al. [20] collated coal pillar detection data from Australia, South Africa, the United States, and other countries and analyzed the strengths of coal pillars under different conditions by using various methods. Petr Wacławik et al. [21] studied the stability of coal pillars by monitoring and analyzing the stress states of coal pillars. Academician Gu Dazhao [22] analyzed the stability of coal pillars in underground reservoirs of coal mines. Song Yimin and Zhang Jie et al. [23,24] analyzed

the deformation field and energy evolution characteristics of coal pillar instability failure and studied the instability characteristics of coal pillars and their overlying rocks. Zhang Cun [25] analyzed the stability of residual coal pillars in underground reservoirs of mines under mining-induced water flooding. Chen Dongdong and Zhao Hongbao et al. [26–28] studied the distribution characteristics of the lateral stress field in coal pillar goaf under different conditions. Tu Min and Wu Baoyang [29,30] used a variety of research methods to study the rational arrangement of coal pillar dams in distributed underground reservoirs of coal mines. In a study on fracture detection, Cao Zhiguo [31] analyzed the distribution model and water flow characteristics of the main channels of water-conducting fractures in mining-induced overlying rocks. Xie Hongxin [32] studied the damage characteristics of water-bearing coal samples under cyclic loading–unloading. Wu Baoyang and Wang Fangtian et al. [33,34] studied the damage and failure law in coal pillar dams under various conditions. Wang Zhenwei [35] numerically analyzed the stress wave propagation law and its influencing factors on coal rock mass. Reed Guy et al. [36] studied the stability of the coal pillar system based on an evaluation method that accounted for the interaction between the coal pillar and the overlying strata. Based on a large number of experimental studies, Yilmaz found that decrease in the friction angle under water infiltration was the main reason for the strength weakening of water-soaked coal rock mass, and that compared with what was found in dry water-soaked coal rock mass, Poisson’s ratio increased while Young’s modulus decreased [37]. Through component analysis and mechanical tests, Verstryne et al. found that the transition from metastable creep failure to accelerated failure in water-soaked sandstone was related to the reaction between water and mineral components [38]. E. Ozdemir et al. found that increase in water content significantly reduced the tensile and compressive strengths of rocks [39].

In the past, the domestic methods of water conservation coal mining were limited height mining, strip mining, and filling mining, all of which affected mining efficiency. For Shandong, with its shallow buried working face with a large mining height, limited mining and strip mining would lead to the waste of coal resources. Large-mining-height filling mining has the disadvantages of high cost and poor effectiveness, while water-preserved coal mining, or the large discharge of mine water, will cause a large amount of evaporation and high loss of water resources, and so underground reservoir technology is the best choice to solve the problem of mine water protection and utilization. With the popularization and application of underground reservoir technology, increasing attention has been paid to the safety of coal pillar dams. Increasing numbers of scholars are studying the coal pillar dams in underground reservoirs of coal mines, but at present, there are few studies on the development and the evolution law of cracks in coal pillar dams and the critical conditions of instability and slip. These factors are key to the safety of coal pillar dams and can determine the optimum size of a coal pillar and the height of water storage while being of great significance to the long-term stable operation of underground reservoirs in coal mines.

Underground reservoirs in coal mines are extremely valuable for the mining industry. They offer an effective way to protect mine water and can reduce the pumping of mine water, save electricity and energy, purify mine water, and realize the green mining of coal. The construction of underground reservoirs in coal mines could reduce global carbon dioxide emissions and the pollution caused by mine water in the environment, effectively contributing to addressing the global climate problem.

The main purpose of this paper is to determine the optimum width of coal pillar dams in the underground reservoir of the Shangwan coal mine so as to reduce and prevent the seepage from the coal pillar dam and improve the safety of underground reservoirs in coal mines.

The research plan of this paper is to analyze the mechanical conditions of crack propagation inside the coal pillar dam under different stress conditions from the perspective of overlying rock pressure and lateral water pressure and study the crack development law and safety of coal pillar dams with different widths, using numerical simulation and similar

simulation, so as to obtain the optimum width of the coal pillar dam in the Shangwan coal mine.

2. The Mechanical Mechanism of Fracture Development and Evolution in the Coal Pillar Dam

The coal rock mass is a complex porous solid, and the primary fractures are formed in the coal rock body due to geological tectonic action; the overlying rock layer on the working face is in equilibrium when mining is not carried out, and the primary fractures exist in isolation. With the remaining of the working face, the original stress balance is broken, and a stress increase zone and stress reduction zones are formed in the coal pillar dam and in the top and bottom plate, respectively, as shown in Figure 1. Stress changes cause primary fractures to propagate and create secondary fractures. As the overlying rock layer on the working face continues to separate, fracture, and balance, the stress is transmitted to the coal pillar dam and to the top and bottom plate so that the stress field also changes. The repeated stress changes make the secondary fractures continue to increase and form a network through each other and then form macroscopic mining cracks [40–42]. If a macroscopic mining fracture has a high degree of development, resulting in the formation of a seepage fracture channel between the underground reservoir of the coal mine and the adjacent roadway outside, the phenomenon of water seepage will result. Therefore, the degree of fracture development in the coal pillar dam is a key factor affecting the safety of underground reservoirs in coal mines, and the fracture development characteristics of the coal pillar dam are inseparable from the stress state in which it is located.

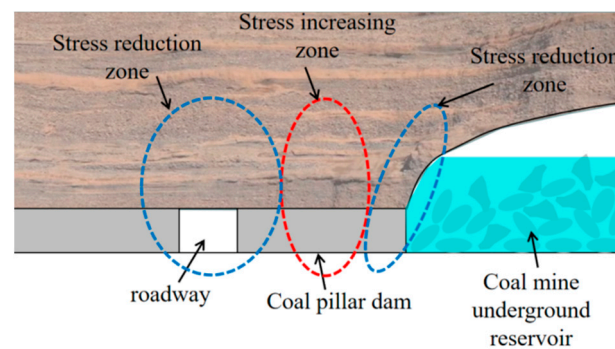


Figure 1. Stress distribution of the coal pillar dam.

In the coal pillar dam's stress increase zone, as the stress increases from the original rock stress to the peak of lateral support pressure, the coal rock mass is subjected to compressive stress. According to the Griffith strength theory, the cracks in the coal rock body propagate due to tensile stress, which is measured by uniaxial tensile strength, R_t , and the strength criterion of fracture propagation is as follows:

$$\begin{cases} \frac{(\sigma_1 - \sigma_3)^2}{8(\sigma_1 + \sigma_3)} \geq R_t & \text{if } \frac{\sigma_3}{\sigma_1} \geq -\frac{1}{3} \\ \sigma_3 = -R_t & \text{if } \frac{\sigma_3}{\sigma_1} < -\frac{1}{3} \end{cases} \quad (1)$$

The angle between the propagation direction of the secondary crack and the long axis of the crack is 2β when $\frac{\sigma_3}{\sigma_1} \geq -\frac{1}{3}$, $\beta = \frac{1}{2} \arccos \frac{\sigma_1 - \sigma_3}{2(\sigma_1 + \sigma_3)}$, and the propagation direction of the secondary crack is parallel to the direction of the long axis of the crack when $\frac{\sigma_3}{\sigma_1} < -\frac{1}{3}$ (Figure 2).

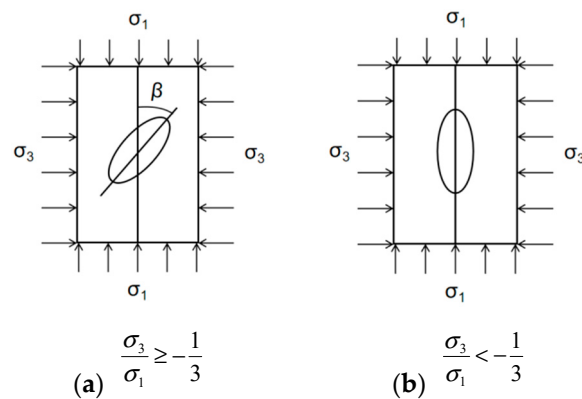


Figure 2. Expansion direction diagram of secondary crack tensile fracture.

In the coal pillar dam’s stress increase zone, when the stress is reduced from the peak of the lateral support pressure to the original rock stress, the lateral pressure change is not obvious, and the vertical stress decreases significantly (this is the pressure relief process; Figure 3). The main form of crack expansion is reverse slip [43], and its critical stress is derived thus:

$$\sigma_1 = \frac{\frac{\sigma_2 \sin 2\theta}{2} - \mu(\sigma_3 - \frac{8G_0\alpha}{k+1}) \cos^2 \theta - 2(\tau_c + \mu\sigma_{1m} \sin^2 \theta)}{\cos \theta \sin \theta + \mu \cos^2 \theta} \tag{2}$$

where μ is the friction coefficient of coal rock, τ_c is cohesion, σ_{1m} is the axial lateral stress at the starting point of unloading, θ is the angle between crack and principal stress direction, and G_0 is the shear modulus of coal rock.

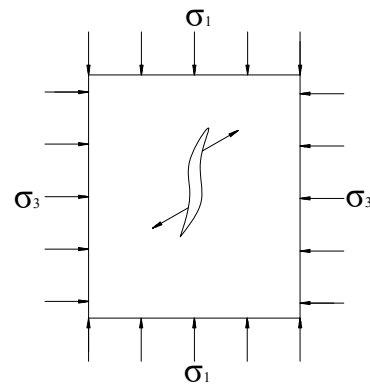


Figure 3. Expansion direction diagram of secondary crack reverse slip.

In the stress reduction zone of the coal pillar dam, the stress is significantly reduced, a large number of secondary fractures are generated by the development of primary fractures, and the secondary fractures of the coal rock mass penetrate due to the tensile-shear composite failure. As shown in Figure 4, the propagations of any two fractures AB and CD produce secondary fractures AF and CE, and the secondary fractures penetrate with tension crack EF to form a fracture network. The penetration strength between fractures is depicted below [44,45]:

$$\sigma_1 = \frac{h\sigma_t(\sin \alpha + f_r \cos \alpha) - 4lc_r + B\sigma_3}{A} \tag{3}$$

where h is the vertical distance between fractures, σ_t is the uniaxial tensile strength of the rock, α is the inclination angle of the tensile crack, f_r is the friction coefficient of the rock, c_r is the rock cohesion, l is the length of the secondary fracture, and A and B are the penetration functions.

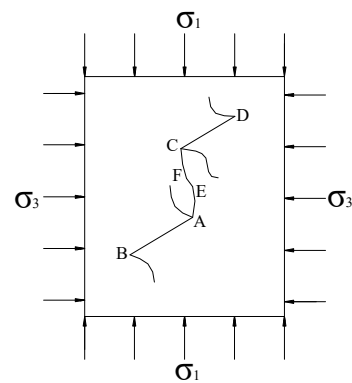


Figure 4. Diagram of transfixion between secondary cracks.

3. Numerical Simulation of Coal Pillar Dam Width in the Shangwan Mine

The special ecological environment of the Shendong area has created the diversity and complexity of the ecological system of the region, and the problem that needs to be solved urgently at this stage is the lack of water resources. However, the coal seam in the Shendong mining area has good storage conditions, large reserves, and a high output, and there is a high loss of surface water and groundwater resources due to the transportation of surrounding rock as a consequence of coal mining, exacerbating the water shortage in the region. Therefore, the utilization of the underground reservoir in the coal mine is an important measure to achieve a win–win situation of energy development and water resource protection and utilization.

The typical underground reservoir of a Shendong coal mine is exemplified in the Shangwan coal mine. The Shangwan coal mine is located in Ejin Horo Banner, Ordos City, Inner Mongolia Autonomous Region, China, and was completed and put into operation in 2000. It covers an area of 61.8 square kilometers and has nine coal seams that can be mined, geological reserves of 1.23 billion tons, recoverable reserves of 830 million tons, an approved production capacity of 16 million tons/year, and a service life of 53 years. The coal is long-flame coal and non-bonded coal, and is a source of high-quality power, coal-to-oil, and chemical and metallurgical coal. The geological structure is simple, and the hydrogeological type is classified as medium. The rock mass of the top and floor of the coal seam in the mining area is of good quality and is relatively complete, but its mechanical strength is low, as it contains mainly weak rocks, and the stability of the top and floor rocks of the coal seam is poor.

3.1. Numerical Simulation Construction and Research Scheme Design of the Underground Reservoir Dam in the Coal Mine

In a study of underground reservoirs, understanding the size and stability of coal pillar dams is the top priority. The general stratigraphic column of the Shangwan coal mine engineering is shown in Figure 5, and the width of the coal pillar dam in the mining process of the UDEC discrete element and the internal stress field, displacement field, and fracture development and change characteristics of the coal pillar dam under the action of lateral water pressure in the goaf area have been constructed by using UDEC discrete elements. This construction has obtained the optimum size of the coal column dam body, providing a theoretical basis for the retention of the coal pillar dam in the Shangwan coal mine.

Based on the general stratigraphic column of the Shangwan coal mine, the numerical simulation is as shown in Figure 6. The model size is defined as length (working face layout direction) \times height (vertical direction) = 236 m \times 280 m, with a 2-2 coal roof plate of 74 m, 2-2 coal seam and 3-1 coal seam spacing 100 m, and 3-1 coal floor of 50 m. The boundary impact area on both sides of the model is of 40 m, the excavation area studied in the middle is of 200 m, and the model contains two layers of coal in the form of 2-2 coal and 3-1 coal. The upper coal seam of 2-2 coal simulates the excavation face in the central area and its two side roadways and the lower coal seam, 3-1 coal, simulates the excavation of

two roadways and one working face on the left and right sides of the central area. The two layers of coal are arranged with 30-m and 15-m coal column dam bodies, respectively, and the spatial relationship between the excavation areas of the upper and lower coal seams is shown in Figure 6.

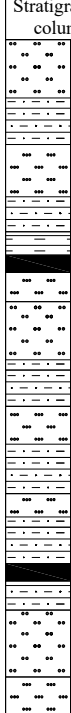
Stratigraphic column	No.	Lithology	Thickness /m
	17	Medium sandstone	20
	16	Sandy mudstone	16
	15	Fine sandstone	18
	14	Sandy mudstone	12
	13	Mudstone	8
	12	2-2 Coal	6
	11	Fine sandstone	10
	10	Medium sandstone	20
	9	Sandy mudstone	16
	8	Fine sandstone	13
	7	Sandy mudstone	17
	6	Fine sandstone	8
	5	Sandy mudstone	16
	4	3-1 Coal	6
	3	Sandy mudstone	10
	2	Medium sandstone	23
	1	Fine sandstone	17

Figure 5. General stratigraphic column of the Shangwan coal mine working face.

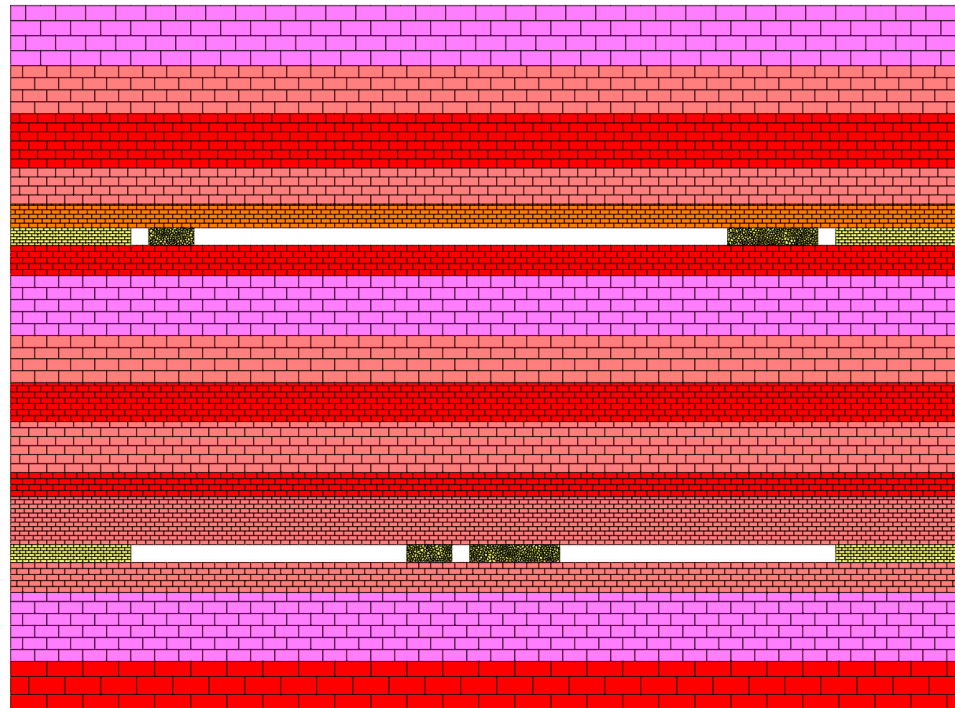


Figure 6. Spatial distribution characteristics of the simulated excavation area.

In order to study the internal variation characteristics of the coal pillar dam, a measuring line with an interval of 1 m is arranged in the middle of the studied coal pillar dam

to monitor its deformation and stress. The objective of the simulation is to excavate 2-2 coal first and then excavate 3-1 coal. Horizontal stress is applied to the 3-1 coal pillar dam to effectively replace the influence of goaf water pressure. During this process, the width and roadway height of the coal pillar dam on the same side of 2-2 coal and 3-1 coal are consistent, and the difference is only limited to the coal pillar dam. There is no lateral horizontal stress. Due to limited space, it is assumed that the optimum coal pillar width for 2-2 coal excavation is equivalent to that for 3-1 coal excavation without lateral horizontal stress. Therefore, the main focus of the simulation study is on the changes of the coal pillar dam body under the conditions of 3-1 coal excavation with horizontal stresses of 0 MPa and 10 MPa.

3.2. Analysis of Simulation Results

(1) Variation characteristics of coal pillar dam body without lateral horizontal stress

From a longitudinal comparison of the distribution of internal stress and deformation under the condition of changing the width of the coal pillar, the vertical stress distribution characteristics and horizontal deformation amount of the coal pillar dam body under only the roof load are obtained using the FISH language as shown in Figures 7 and 8. Figure 7 shows that the widths of the left coal pillar are 15 m, 20 m, and 25 m, respectively, from top to bottom, and the widths of the right coal pillar are 30 m, 35 m, and 40 m, respectively. From the horizontal deformation amount of the coal pillar, it can be concluded that as the size of the coal pillar decreases, the deformation amount on both sides of the coal pillar shows an increasing trend, with a large increment on the free side of the coal pillar and a small increment on the roadway side of the coal pillar. The internal deformation amount of the 15–25-m coal pillar increases approximately linearly, while the internal deformation amount of the 30–40-m coal pillar is basically consistent and small. By dividing the deformation amount by using a color scale and analyzing the range of coal pillar deformation using color scale area of displacement of less than 0.1 m as a reference, it can be concluded that the corresponding areas of coal pillars that are of 15 m, 20 m, 25 m, 30 m, 35 m, and 40 m are 0 m, 5 m, 10 m, 17 m, 22 m, and 29 m, respectively, accounting for 0%, 25%, 40%, 57%, 62%, and 72% of coal pillar width, respectively. The proportion of this area increases with the increase in coal pillar width, with increments of 25%, 15%, 17%, 5%, and 10%, respectively. From these results, it can be concluded that the stable area inside the coal pillar under the condition of 30 m has a larger increment compared to under the conditions of 25 m and 35 m. From the perspective of the distribution characteristics of vertical stress inside the coal pillar, it can be seen that the vertical stress on the left and right sides of the coal pillar increases as the size of the coal pillar decreases. Between them, the vertical stress peak value of the 30-m coal pillar is the highest and the bearing stress is the largest. Considering that the internal deformation of the coal pillar is small, it can be concluded that the 30-m coal pillar has the optimal size of the coal pillar dam.

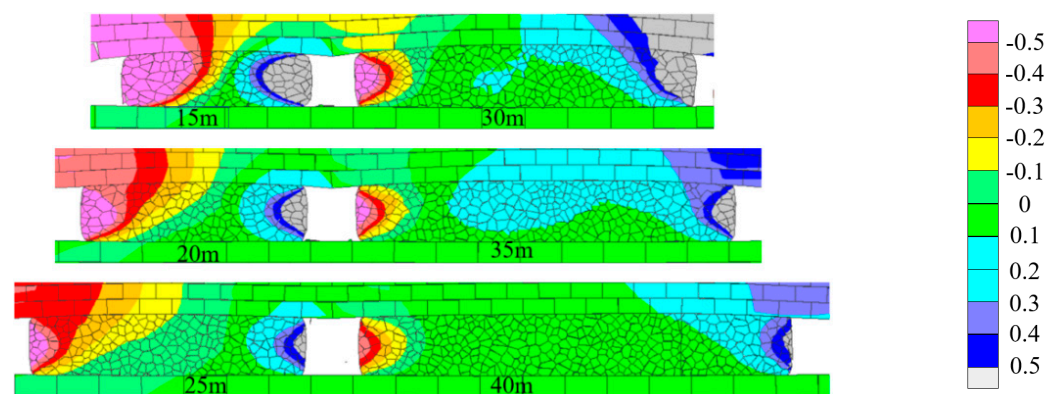
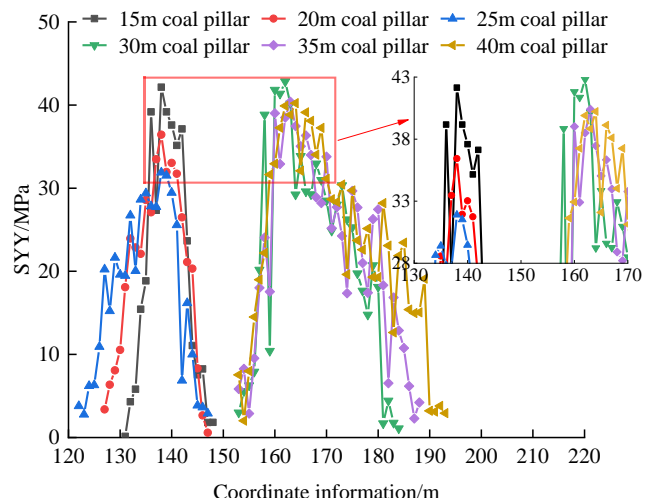
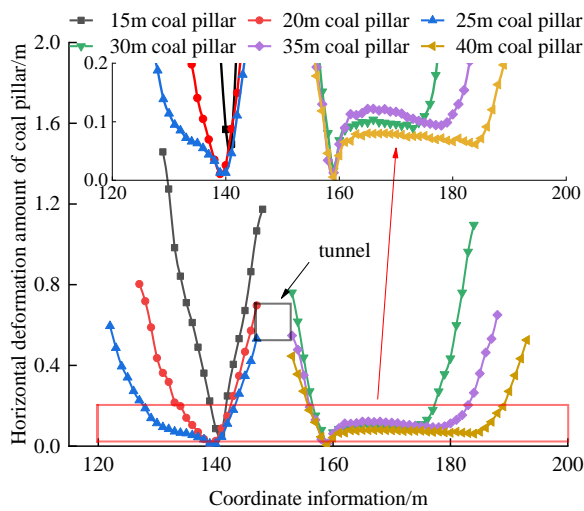


Figure 7. Cloud Chart of Horizontal Displacement of Coal Pillar Dam/m.

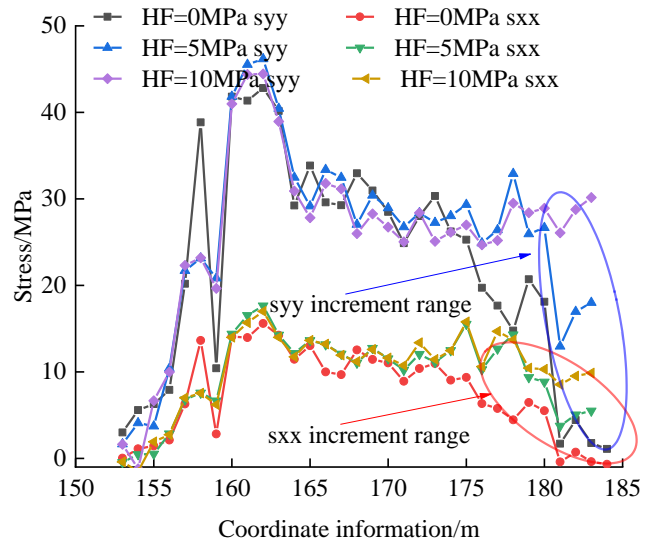
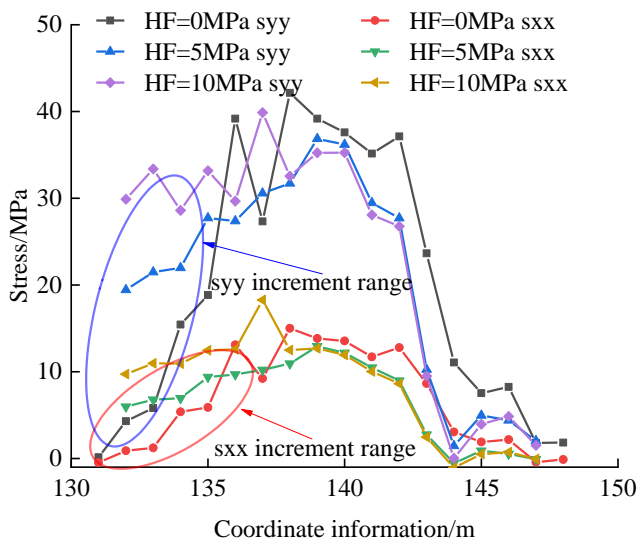


(a) Horizontal displacement of measuring point (b) Vertical stress distribution characteristics of measuring point

Figure 8. Change characteristics of a coal pillar dam body without lateral horizontal stress.

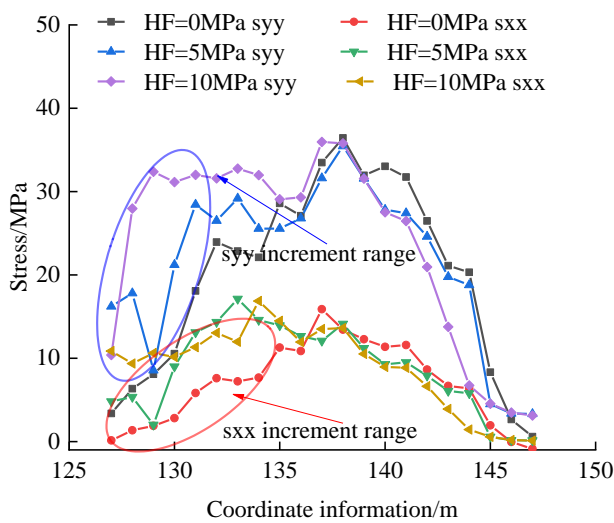
(2) Variation characteristics of coal pillar dam considering lateral horizontal stress

Based on the above pressure variation characteristics of coal pillar dams without horizontal lateral pressure, it is necessary to supplement the variation characteristics of coal pillar dam stability under goaf water filling conditions in order to further study the stability of coal pillar dams in underground reservoirs. Due to the large amount of data from multiple groups of comparative analysis, when analyzing only 15 m and 30-m coal pillars, horizontal stress is applied to both sides of the 3-1 coal seam, and the variation rules of s_{xx} and s_{yy} stresses under the conditions of 0 MPa, 5 MPa, and 10 MPa are shown in Figure 9.

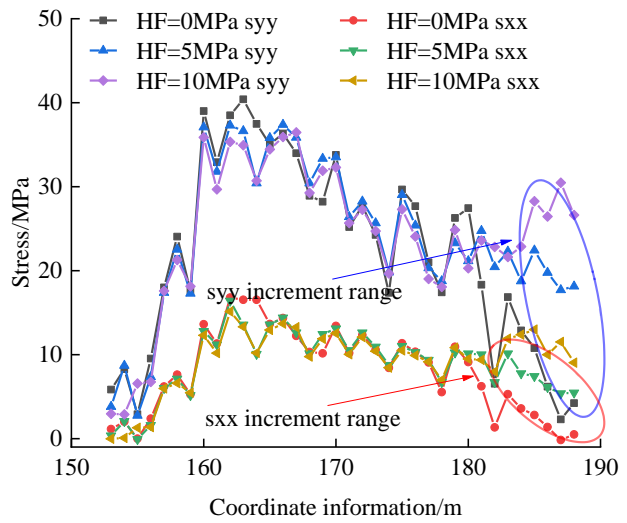


(a) Under the condition of 15-m coal pillar (b) Under the condition of 30-m coal pillar

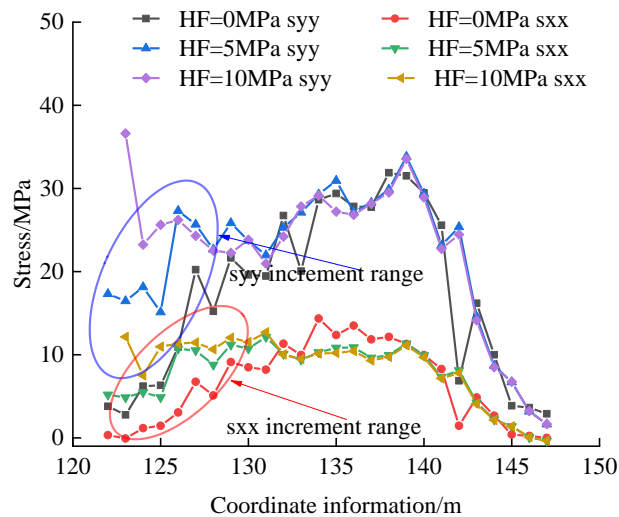
Figure 9. Cont.



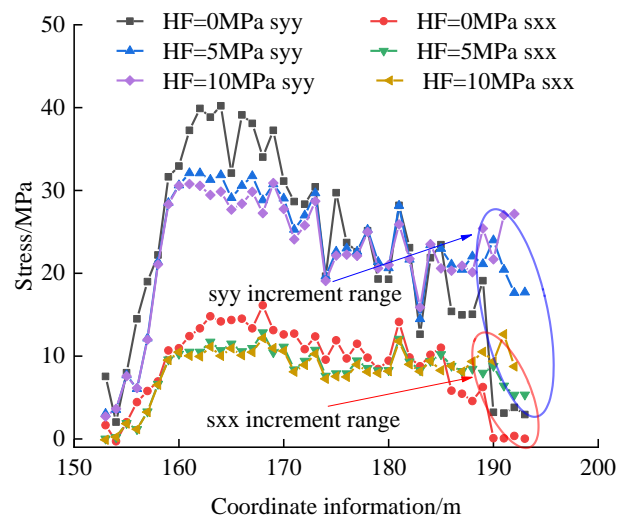
(c) Under the condition of 20-m coal pillar



(d) Under the condition of 35-m coal pillar



(e) Under the condition of 25-m coal pillar



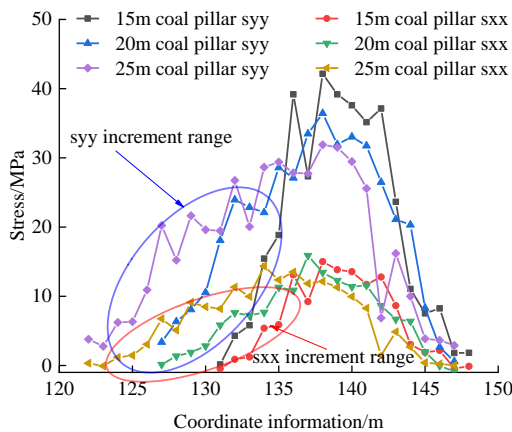
(f) Under the condition of 40-m coal pillar

Figure 9. The influence of the change in the width of the coal pillar dam on its stress variation characteristics.

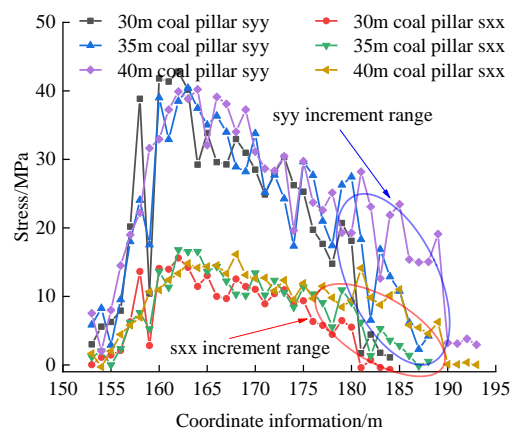
As shown in Figure 9, under the action of horizontal stress applied to the goaf side of the coal pillar dam, the stress of s_{yy} and s_{xx} on the goaf side of the coal pillar dam, which is positively correlated with the horizontal stress, increases. The smaller the size of the coal pillar is, the greater the increment of stress in s_{yy} and s_{xx} is. After comparing and analyzing the differences in the changes of coal pillar s_{yy} and s_{xx} under the action of horizontal stress, it can be concluded that horizontal force has an impact on the stability of coal pillars. With the increase in coal pillar width, the influence range of horizontal force on the goaf side of the coal pillar dam becomes smaller and smaller. When the coal pillar width is 15 m or 20 m, the application of horizontal stress causes changes in s_{xx} and s_{yy} in all areas inside the coal pillar, thus indicating that horizontal force is transmitted from the goaf side to the roadway side. Horizontal force has a significant impact on the stress state of the coal pillar, indicating that the stability and bearing capacity of the coal pillar decrease under the action of horizontal force. When the width of the coal pillar is 25–40 m, the variation areas of the s_{yy} of the coal pillar after the horizontal force is applied are 12 m, 8 m, 8 m, and 7 m, and for those values, the s_{xx} variation areas are 16 m, 10 m, 8 m, and 7 m, respectively. Considering the influence range of the horizontal force on the

coal pillar stress in the goaf side when the width of the coal pillar is 30–40 m, it can be found that the influence range of the horizontal force on the coal pillar is basically the same. When the width of the coal pillar is 30 m, the influence of the horizontal force on the coal pillar on the goaf side no longer changes significantly. From the comparison of the bearing capacity and stress state of the coal pillar, it can be concluded that a coal pillar of 30 m is the optimum width.

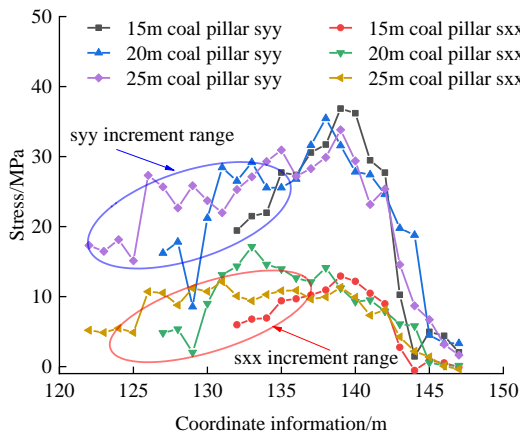
As shown in Figure 10, by comparing the internal stress variation characteristics of 15–25 m and 30–40-m coal pillars under the same horizontal force conditions, when there is no horizontal stress on the coal pillar dam body, the fluctuation range of s_{yy} and s_{xx} stress in the middle area of both coal pillars and the side of the goaf is relatively large. When a 5-MPa horizontal stress is applied to the goaf side of the coal pillar dam, the fluctuation range of s_{yy} and s_{xx} stress in the middle area of the 15–25 m and 30–40-m coal pillars and the side of the goaf is significantly reduced. When a 10-MPa horizontal stress is applied to the goaf side of the coal pillar dam, the s_{yy} and s_{xx} stresses in the middle areas of the 15–25 m and 30–40-m coal pillars and the side of the goaf are similar. The coal pillar width of 15–25 m is significantly larger than the area affected by the horizontal force of 30–40-m coal pillars. Therefore, when the horizontal stress on the side of the gob of the coal pillar dam increases, the smaller the coal pillar width is, the greater the stress change on s_{yy} and s_{xx} on the side of the gob of the coal pillar dam becomes. Therefore, as the horizontal stress increases, the size of the coal pillar decreases, and the stress increment of s_{yy} and s_{xx} becomes more significant. The goaf side of the coal pillar is the starting point for the stress increment of s_{yy} and s_{xx} . The larger the stress increment is, the more easily the coal pillar is damaged, indicating that small coal pillars are more sensitive to horizontal pressure.



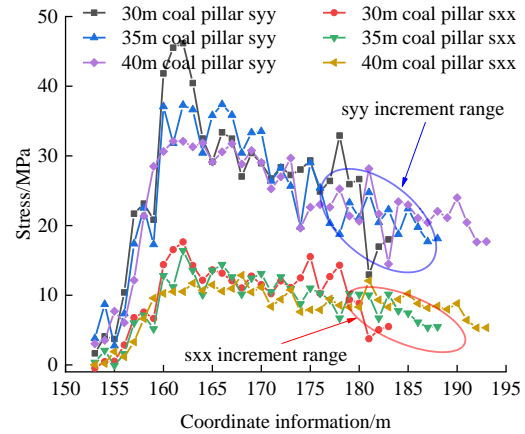
(a) 15–25-m coal pillar without horizontal stress



(b) 30–40-m coal pillar without horizontal stress

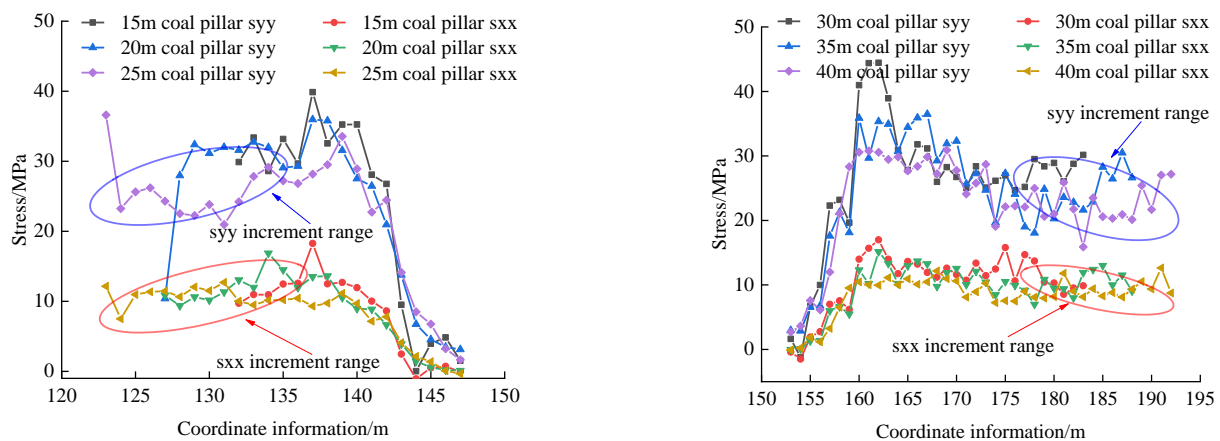


(c) Horizontal stress of 15–25-m coal pillar = 5 MPa



(d) Horizontal stress of 30–40-m coal pillar = 5 MPa

Figure 10. Cont.



(e) Horizontal stress of a 15–25-m coal pillar = 10 MPa (f) Horizontal stress of a 15–25-m coal pillar = 10 MPa

Figure 10. Stress variation characteristics of a coal pillar dam body under lateral horizontal stress conditions.

4. Experimental Study on Crack Development in a Coal Pillar Dam

Based on the numerical simulation results for crack development in a coal pillar dam body of different sizes in the Shangwan mine, the coal pillar dam is of the best size when the width of the coal pillar is 30 m. In this section, similar simulation experiments that were used to study coal pillar dams with two widths—30 m and 15 m—are described.

4.1. Similar Simulation Experiment Research Scheme

This simulation experiment, which is similar to the previous one, analyzed the macroscopic fracture development in and slip instability characteristics of a coal pillar dam under different stress conditions and used the “Multi-seam Mining Coal Mine Underground Reservoir Simulation Test Platform” to carry out the relevant experiments. Above this platform are seven servo motors, which can load vertical force, that can simulate the self-weight of the overlying strata and achieve local loading, and two servo motors, which can load horizontal force, that can simulate the lateral water pressure of underground reservoirs of coal mines. The simulation test platform can be laid on a simulation test platform with dimensions of 2100 mm × 1800 mm × 300 mm. The similarity ratio of this experiment was 1:150, and the physical and mechanical parameters of each rock layer were consistent with the numerical simulation parameters. In this simulation, the process of mining a 2-2 coal face and a 3-1 coal face in Shangwan coal mine and forming an underground reservoir was simulated. The two layers of coal were arranged with coal pillar dams of 30 m and 15 m, respectively. As shown in Figure 11, the 2-2 coal layout had a 178-m-wide working face and a 15 m and a 30-m coal pillar dam body were arranged on both sides. The 3-1 coal layout had two 132-m working faces, and the two adjacent coal pillar dam bodies, which were of 15 m and 30 m, were arranged in the middle.

In order to monitor the stress change characteristics inside the coal column dam, a coordinate system was established, with X in the transverse direction and Y in the longitudinal direction, and the stress measurement points were arranged. The scheme, as shown in Figure 12, indicated that one stress measuring point in the Y direction was uniformly arranged inside the two coal pillars of 2-2 coal seam along the X direction, and two stress measuring points in the Y direction were uniformly arranged at the upper boundary along the X direction (Figure 12a,b). One stress measuring point in the X direction was uniformly arranged inside the two coal pillars of 3-1 coal along the Y direction, and one stress measuring point in the Y direction was arranged at the upper boundary (Figure 12c,d).

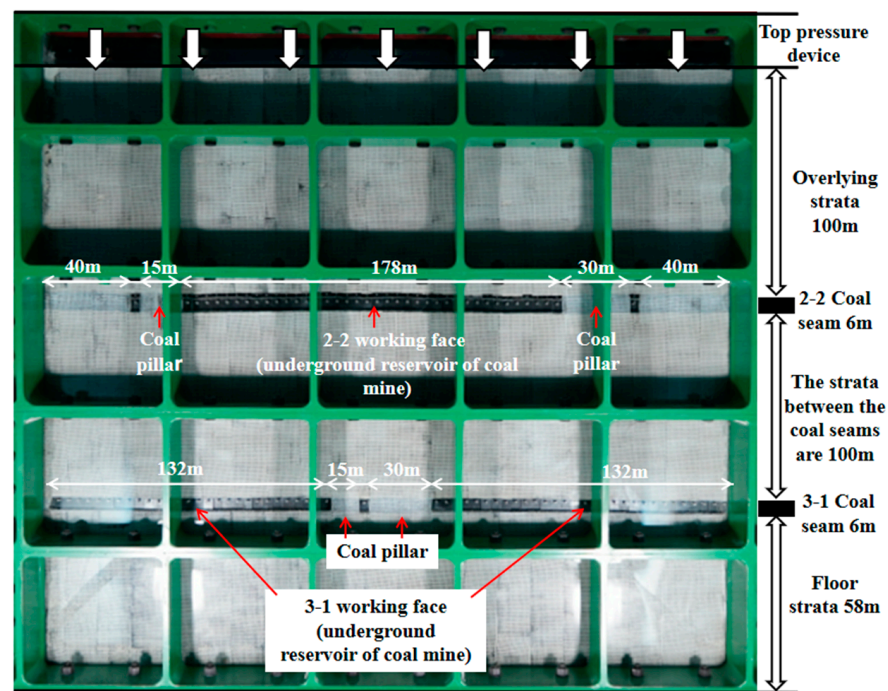


Figure 11. Similar simulation experiment scheme.

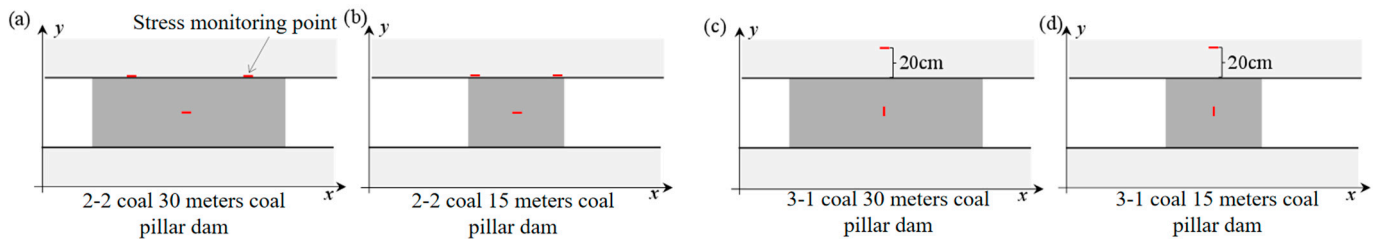


Figure 12. Arrangement of stress monitoring points of a coal pillar dam.

4.2. Analysis of the Fracture Development Characteristics of a Coal Pillar Dam under the Stress of Overlying Strata

In order to analyze the vertical bearing capacities of coal pillar dams of different sizes, after mining the 2-2 coal seams, the load was applied on top of the two coal pillars. The stress monitoring sheet embedded in the coal column was used to monitor the stress of the coal pillar dam and its top and bottom plate. A high-definition camera was used to take regular pictures of the surface of the coal pillar dam to monitor the development characteristics of and displacement of cracks on the surface of the coal pillar dam. According to the observation results of stress, displacement, and fracture development, the fracture development evolution law and the failure instability characteristics of the coal pillar dam were further analyzed.

(1) Analysis of the stress failure characteristics of a 15-m 2-2 coal pillar

The overlying rock layer of the 2-2 coal 15-m coal pillar was locally compressed, as shown in Figure 13; the stress inside the coal pillar and the top monitoring point increased linearly with the increasing upper load. When the stress of the monitoring point adjacent to the reservoir side at the top of the coal pillar reached 0.62 MPa, the stress value dropped sharply, and no obvious damage occurred on the roadway side, while the roof plate of the reservoir side was completely destroyed, resulting in the stress loss of pressure at the monitoring point. The stress at the monitoring points inside the coal pillar and adjacent to the roadway side at the top continued to fluctuate and increase linearly, and subsequently showed the characteristics of slow growth, during which the original fracture of the coal

pillar dam expanded and the fracture opening and length increased. When the stress of the monitoring point reached 0.69~0.73 MPa, the cracks between the top and bottom plates of the coal pillar dam (reservoir side) gradually expanded and penetrated each other. When the stress of the monitoring point reached 0.78~0.89 MPa, the coal body of the coal pillar dam (reservoir side) formed a semi-oval spalling body, which was separated from the coal pillar, and the crack could be observed macroscopically at up to about 5 mm. The coal body on the other side of the roadway also produced long cracks that ran through the top and bottom plates and basically formed a semi-oval spalling. When the stress of the monitoring point reached 0.85~0.91 MPa, the coal body of the coal pillar dam (reservoir side) had a wall caving, which was completely scattered in the roadway, and the coal body spalling on the other side was separated from the coal pillar, forming a crack of about 4 mm. When the stress of the monitoring point reached 0.96~1.04 MPa, the coal body on both sides of the roadway had a wall caving, and after cleaning the roadway, it could be seen that the effective support width of the coal pillar dam was getting smaller, and the stress of the monitoring point also tended to be stable, and the coal pillar dam recovered stability. With the continuous increase in the upper load, the stress at the monitoring point suddenly dropped sharply from 0.9 MPa directly to approximately 0.3 MPa.

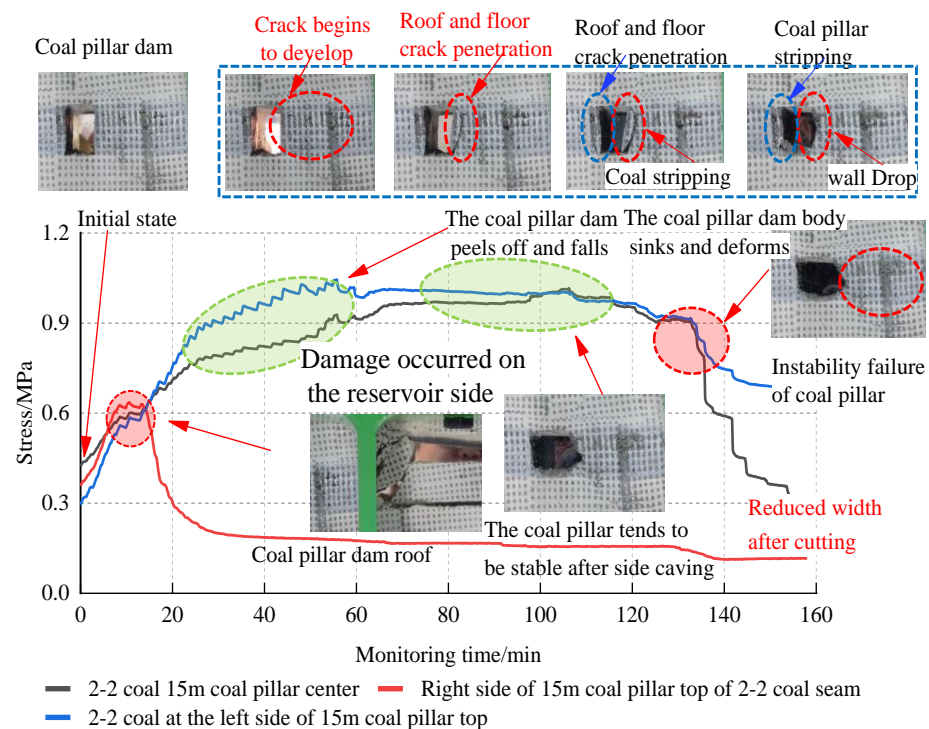


Figure 13. Stress failure characteristics of a 15-m coal pillar of 2-2 coal.

As shown in Figure 14, externally, the coal pillar dam produced obvious deformation, indicating that at this time, the internal cracks of the coal pillar dam had a high degree of development. The internal structure had been completely destroyed, as it could not bear the load of the overlying rock layer, and the load was transmitted to the outer coal pillar and the gravel in the reservoir, so far indicating that the coal pillar was unstable and damaged. The final effective bearing width of the coal pillar dam body was 11.5 m.

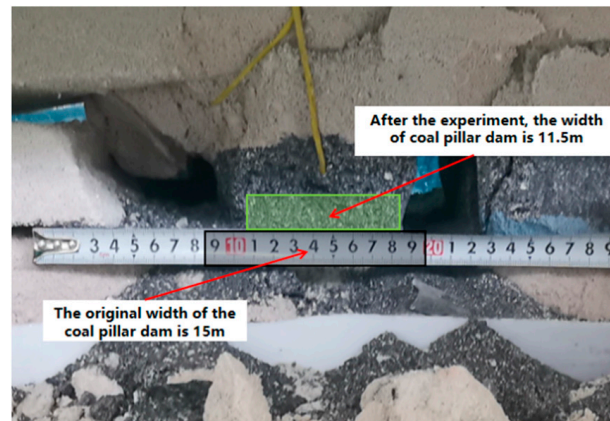


Figure 14. Final width of the coal pillar dam after instability and failure.

(2) Analysis of stress failure characteristics of a 30-m 2-2 coal pillar

The overlying rock layer of the 30-m coal pillar of 2-2 coal was locally compressed, as shown in Figure 15, and the stress in the internal and top monitoring points of the coal pillar dam increased linearly over a period of time. After reaching 0.62–0.69 MPa, with the continuous increase in the upper load, the stress of the monitoring point did not change significantly, and after a long time until the upper unloading, obvious cracks and wall caving did not appear in the coal pillar. Only a certain deformation appeared in the coal pillar. These results showed that the 30-m coal pillar could remain stable for a long time under the state of top pressure, that it did not strip the wall caving, and that its bearing capacity was better than that of the 15-m coal pillar. The increase in the width of this coal pillar weakened the stress concentration benefit, the coal pillar was not easily “eroded” by stress and cracks, the overall bearing capacity was enhanced, and the coal pillar dam was safer.

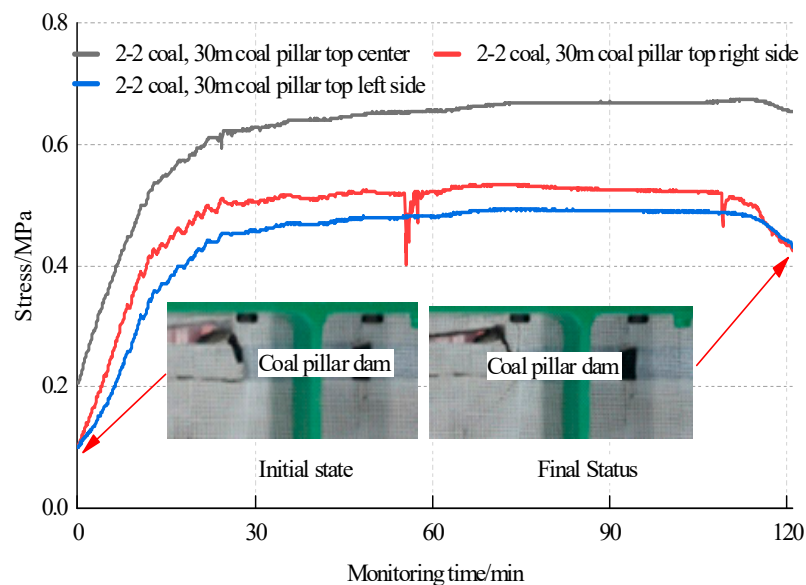


Figure 15. Stress failure characteristics of a 30-m coal pillar of 2-2 coal.

(3) Analysis of the crack development characteristics of a coal pillar dam

According to the experimental results, the fracture development characteristics of the 15-m coal pillar dam of the 2-2 coal seam were more obvious. Therefore, taking the 15-m coal pillar dam body of the 2-2 coal seam as an example, the digital image processing and analysis technology DAVIS was used to further analyze the fracture development characteristics of the coal pillar dam under vertical load conditions. As shown in Figure 16, under

the vertical load at the top, the coal pillar dam body went through four stages—fracture generation, propagation, roadway roof failure, and coal pillar dam damage—from the initial stage before compression. In the fracture generation stage, with the increasing pressure at the top, cracks began to appear in the top corner and floor of the roadway of the coal pillar dam. In the fracture propagation stage, visible cracks also appeared directly above the roadway, and cracks were generated in the middle of the coal pillar. In the stage of roof failure of the roadway, cracks appeared continuously in the top rock mass, flakes appeared at the top corner, and cracks in the middle of the coal pillar gradually developed towards the bottom corner. In the damage stage of the coal pillar, the roof plate collapsed sporadically, the coal pillar appeared to have wall caving, the crack expanded to the upper rock formation of the roadway, and the crack in the coal pillar developed and extended to the side of the goaf.

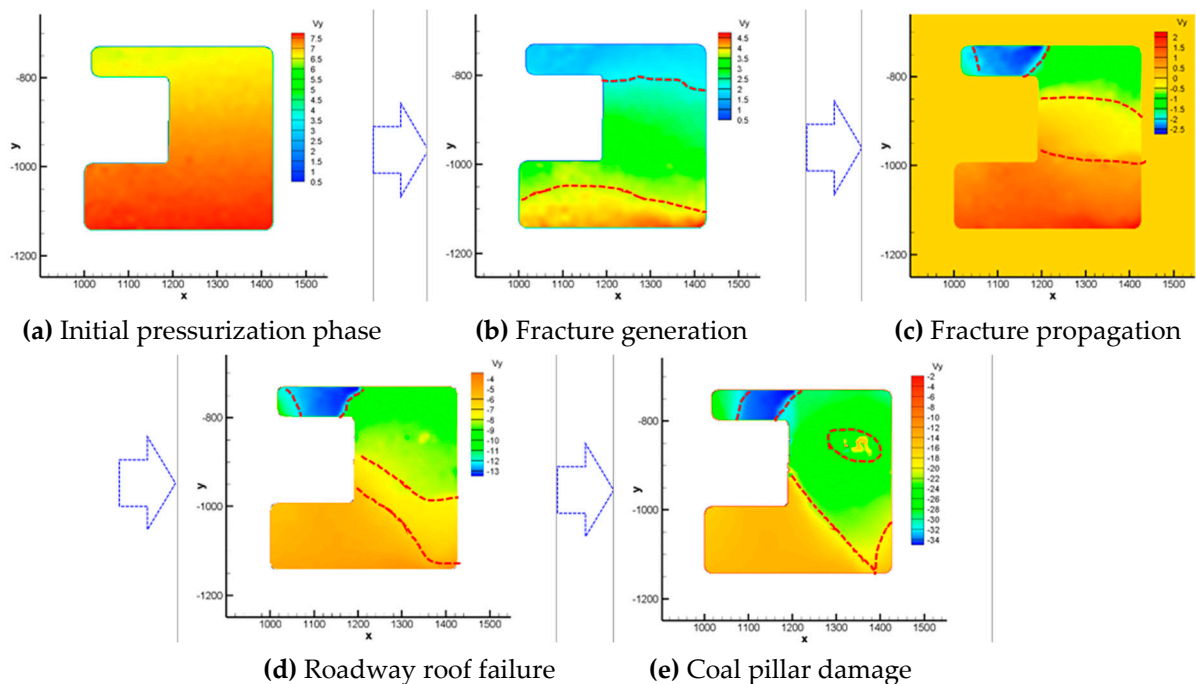


Figure 16. Characteristics of crack development in a coal pillar dam.

Based on the above analysis, the following points can be noted. (1) The smaller the size of a coal pillar dam is, the smaller the pressure that can carry the overlying rock layer is, the easier it is to form a stress concentration area in the coal pillar, and the more likely the stress concentration benefit is to produce the phenomenon of an “eroded” coal pillar, resulting in a decrease in the coal pillar’s effective width. (2) According to the experimental results, after the continuous compression of the coal pillar dam, the roof plate near the reservoir side is the first to be damaged, followed by the coal body on the roadway side. Then, the crack development degree of the coal pillar dam increases and the smaller size of the coal pillar will eventually become damaged. (3) The larger the size of the coal pillar dam is, the less obvious the stress concentration effect is and the stronger its bearing capacity is; moreover, there is no obvious stripping of the wall caving, thus ensuring the long-term safe operation of the reservoir.

4.3. Analysis of the Fracture Development Characteristics of a Coal Pillar Dam under the Dual Action of the Overlying Rock Layer and Lateral Water Pressure

In order to analyze the lateral bearing capacities of different sizes of coal pillar dam, after mining in 3-1 coal seams, the lateral load was applied to two coal pillars to simulate the lateral water pressure. The linear displacement sensor was used to monitor the horizontal displacement of the coal pillar, and the surface of the coal pillar dam was photographed

regularly to monitor the fracture development characteristics of the coal pillar dam. According to the observed results of applied load, displacement, and fracture development, the fracture development and evolution law and the failure slip characteristics of the coal pillar dam were further analyzed.

(1) Analysis of the stress-failure slip characteristics of a 15-m 3-1 coal pillar

The lateral load was applied to the 15-m coal pillar of 3-1 coal, and the displacement of the roadway outside the coal pillar dam was recorded. As shown in Figure 17, after the loading started, the load increased linearly, but the amount of displacement was always 0. After loading for 5 min, the load did not increase, and was stable at about 480 kg. At this time, which was the elastic deformation stage, the coal pillar dam had not yet been displaced. When loading was done for approximately 6 min, the crack began to develop and the coal pillar produced obvious deformation. At the same time the coal pillar produced horizontal displacement, which increased linearly. When loading was done for approximately 12 min, the load suddenly decreased, and then the displacement also stopped at 9.15 mm. At this point, the coal pillar crack had been highly developed for the plastic failure stage, and the coal pillar roof plate had obvious separation cracks. When loaded to 23 min, the load dropped abruptly again, the coal pillar displacement suddenly increased linearly, and the coal pillar dam body was unstable and slipped.

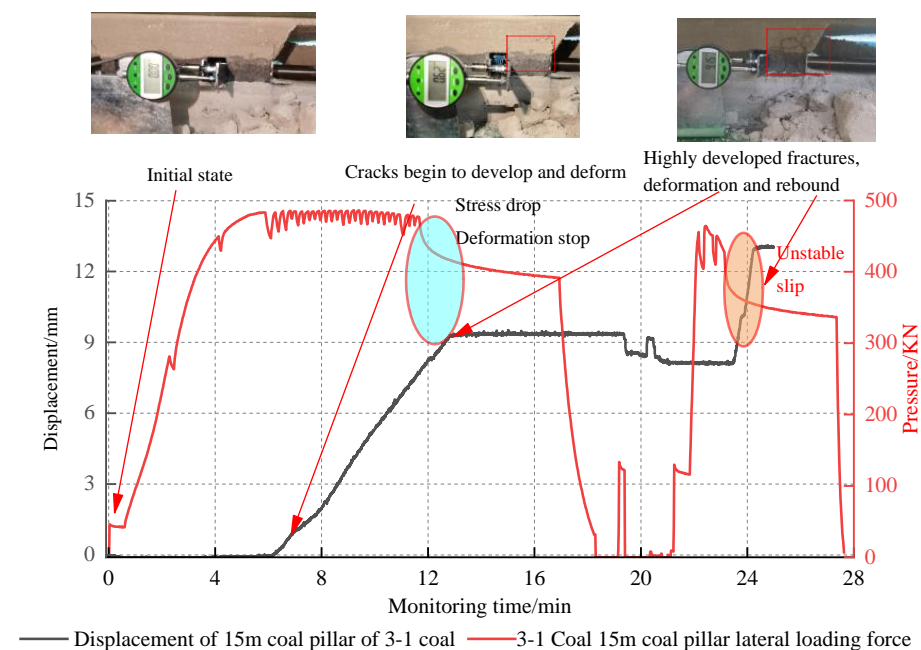


Figure 17. Stress failure characteristics of a 15-m coal pillar of 3-1 coal.

(2) Analysis of stress-failure slip characteristics of a 30-m 3-1 coal pillar

We apply the load laterally to the 30-m coal pillar of 3-1 coal. As shown in Figure 18, after the start of loading, the load increased in volatile linear growth, but the amount of displacement was always 0. After 10 min of loading, the load reached a peak of approximately 1250 kg, after which the coal pillar dam was displaced; this was the elastic deformation stage. When the displacement reached about 7 mm, the crack of the roof of the coal pillar dam had been preliminarily penetrated and the coal pillar had obvious deformation. Within 10–12 min of loading, the load continued to decrease, and the displacement increased linearly with a large increase; this was the plastic failure stage. When loaded to 12 min, the load dropped, the coal pillar dam suddenly slipped and became unstable, and the cracks between the top and bottom plates of the coal pillar had been completely penetrated.

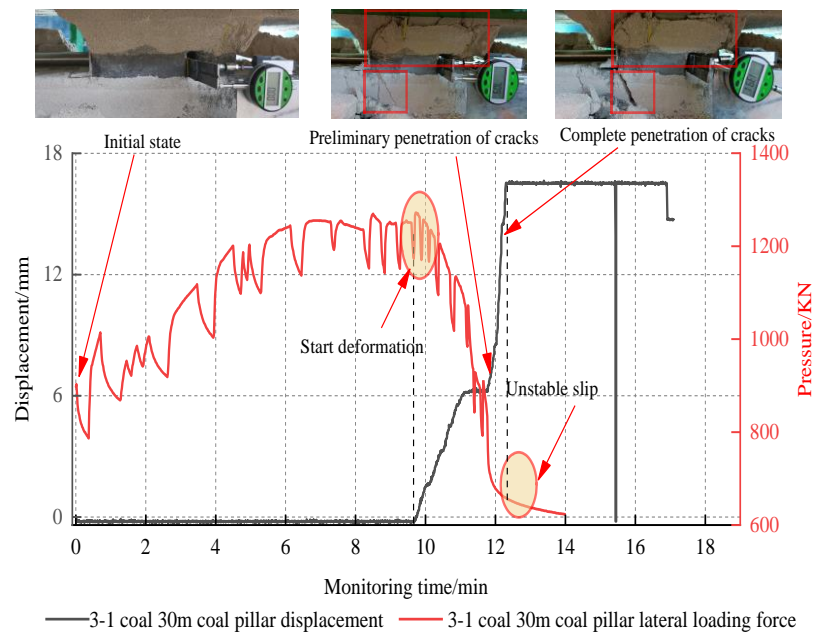


Figure 18. 3-1 Stress failure characteristics of a 30-m coal pillar.

Based on the above analysis, the following can be seen: (1) The size of a coal pillar dam is proportional to the lateral maximum water pressure it can bear. (2) Under the action of lateral water pressure, the coal pillar dam undergoes the process of “elastic deformation–plastic failure–instability slip”, and the fracture develops most rapidly in the plastic failure stage—generally until the top and bottom plate cracks are completely penetrated—and instability slip occurs. (3) Experimentally, the maximum water level that the coal pillar dam can withstand can be roughly determined. For example, the maximum water level that can be withstood by a 15-m coal pillar is 50 m, which is the safe water storage height.

5. Conclusions

In this paper, the fracture evolution law and the critical conditions of failure instability of a coal pillar dam under different load conditions were studied, and the optimum size and safe water storage height of coal pillar dams were studied by establishing mechanical models, numerical simulations, and similar simulations. The following conclusions were obtained:

- (1) The smaller the size of the coal pillar dam is, the smaller the pressure of the overlying rock layer is, and thus, the easier it is to form a stress concentration area in the coal pillar. Here, the stress concentration benefit is more likely to cause the coal pillar to be “eroded,” resulting in a decrease in its effective width. The larger the size of the coal pillar dam is, the less obvious the stress concentration effect is and the stronger its bearing capacity is, and there is no obvious stripping phenomenon, thus ensuring the long-term safe operation of the reservoir.
- (2) According to the experiment that used a similar simulation, the process of being “eroded,” for the 15-m coal pillar dam in Shangwan coal mine, was as follows. First, with the increase in stress, obvious cracks first appeared in the roof and floor of the roadway, extending to the interior of the coal pillar dam until the cracks in the roof and floor were connected, forming a semi-elliptical coal body in the coal pillar dam body and separating from the coal pillar dam body. Subsequently, the wall spalling and the width of the coal pillar dam body reduced. The “eroded” process would be repeated many times during the operation of the coal pillar dam, and so it could be noted that the safety of small coal pillars is not as effective as that of large coal pillars.
- (3) The size of the coal pillar dam is proportional to the lateral maximum water pressure it can bear. The coal pillar dam undergoes the process of “elastic deformation–plastic

damage–instability slip” under the action of lateral water pressure. By using the experimental method, the maximum water level that the coal pillar dam can withstand can be roughly determined. The maximum water level that a 15-m coal pillar can withstand in the Shangwan coal mine is 50 m, which is the safe water storage height.

- (4) Through interpreting the results of numerical simulation, it was determined that the optimal size of a coal pillar dam in the Shangwan mine is 30 m, and that the fracture development of the coal pillar at this size does not penetrate inside and outside the reservoir under the action of the overlying rock layer and lateral water pressure, thus ensuring the long-term safe operation of the underground reservoir in the coal mine.

6. Future Prospects and Possible Research Directions

Underground reservoirs in coal mines are an effective means to develop China’s coal mining in the direction of environmental protection. They not only reduce the waste of water resources and carbon dioxide emissions, but also save costs and improve the economic benefits of coal mines. In this paper, one of the factors affecting the stability of coal pillar dams in underground reservoirs of coal mines has been discussed: that is, the development and the evolution law of fissures, and some useful suggestions on the size of coal pillars, have been put forward. Future research on underground reservoirs in coal mines may be directed toward the following topics:

- (1) Theoretical aspects: investigating (i) whether coal mining causes the coal mine water migration law in overburden rock, (ii) the purification mechanisms and effectiveness of underground reservoirs in coal mines, and (iii) whether the underground reservoirs in coal mines affect the stability of sewage systems and water inflow prediction;
- (2) Construction technology: in-depth research on the construction technology used for underground reservoirs in coal mines under complex geology, large burial depth, high gas levels, rock burst, and other conditions;
- (3) Construction technology: the artificial dam body and its joint may easily produce mine water leakage. The construction of the artificial dam body should be improved, and appropriate grouting or anti-seepage materials to ensure an anti-seepage effect at the joint should be researched and developed;
- (4) Safety monitoring system: no systematic safety evaluation system has been established for underground reservoirs of coal mines. Monitoring equipment and integrated systems for underground reservoirs in coal mines need to be developed and a scientifically proven and safe monitoring system needs to be established.

Author Contributions: Conceptualization, B.Z.; Methodology, B.Z. and W.N.; Investigation, B.Z. and X.H.; Writing—original draft, B.Z., W.N. and H.L.; Formal analysis, B.Z., H.L. and Y.S.; Writing—review and editing, B.Z. and H.L. All authors have read and agreed to the published version of the manuscript.

Funding: This research received no external funding.

Institutional Review Board Statement: Not applicable.

Informed Consent Statement: Not applicable.

Data Availability Statement: The data used to support the findings of this study are available from the corresponding author upon request.

Conflicts of Interest: The authors declare no conflict of interest.

References

1. Dong, S.; Xu, B.; Yin, S.; Han, Y.; Zhang, X.; Dai, Z. Technology and engineering development strategy of water protection and utilization of coal mine in China. *J. China Coal Soc.* **2021**, *46*, 3079–3089.
2. Zhang, G.; Li, Q.; Xu, Z.; Zhang, Y. Roof Fractures of Near-Vertical and Extremely Thick Coal Seams in Horizontally Grouped Top-Coal Drawing Method Based on the Theory of a Thin Plate. *Sustainability* **2022**, *14*, 10285. [[CrossRef](#)]
3. Yan, J.; Zhang, X.; Wang, K.; Song, X.; Yue, S.; Hou, J. Experimental Study on Creep Characteristics and Long-Term Strength of Anthracite. *Processes* **2023**, *11*, 947. [[CrossRef](#)]

4. Wang, X.-H.; Zhang, H.-H.; Wu, Z.; Li, X.-L.; Sui, Y.; Gao, R.-Q. Selection and Optimization Mechanism of the Lower Return Roadway Layout in the near Residual Coal Pillar Area. *Processes* **2022**, *10*, 2471. [[CrossRef](#)]
5. Shi, X. Research progress and prospect of underground mines in coal mines. *Coal Sci. Technol.* **2022**, *50*, 216–225.
6. Yu, Y.; Ma, L. Application of roadway backfill mining in water-conservation coal mining: A case study in northern shaanxi, China. *Sustainability* **2019**, *11*, 3709. [[CrossRef](#)]
7. Ju, J.; Xu, J.; Li, Q.; Zhu, W.; Wang, X. Progress of water—Preserved coal mining under water in China. *Coal Sci. Technol.* **2018**, *46*, 12–19.
8. Gu, D.; Zhang, J. Modern Coal Mining Affected to Underground Water Deposit Environment in West China Mining Area. *Coal Sci. Technol.* **2012**, *40*, 114–117.
9. Xiong, Z.; Wang, L. The Pollution Status of Ground Water and Treatment Methods in China. *World Sci. Res. J.* **2021**, *7*, 227–232.
10. Gu, D. Theory framework and technological system of coal mine underground reservoir. *J. China Coal Soc.* **2015**, *40*, 239–246.
11. Gu, D. Water Resource Protection and Utilization Engineering Technology of Coal Mining in “Energy Golden Triangle” Region. *Coal Eng.* **2014**, *46*, 34–37.
12. Gu, D.; Zhang, Y.; Cao, Z. Technical progress of water resource protection and utilization by coal mining in China. *Coal Sci. Technol.* **2016**, *44*, 1–7.
13. Pang, Y.; Li, P.; Zhou, B. Underground reservoir construction technical feasibility analysis in 8.0m large mining height working face. *Coal Eng.* **2018**, *50*, 6–15.
14. Unver, B.; Yasitli, N.E. Modelling of strata movement with a special reference to caving mechanism in thick seam coal mining. *Int. J. Coal Geol.* **2006**, *66*, 227–252. [[CrossRef](#)]
15. Zhang, G.; Li, Q.; Zhang, Y.; Du, F. Failure characteristics of roof in working face end based on stress evolution of goaf. *Geomech. Geophys. Geo-Energ. Geo-Resour.* **2021**, *53*, 7. [[CrossRef](#)]
16. Singh, R.; Mandal, P.K.; Singh, A.K.; Singh, T.N. Cable-bolting-based semi-mechanised depillaring of a thick coal seam. *Int. J. Rock Mech. Min. Sci.* **2001**, *38*, 245–257. [[CrossRef](#)]
17. Zhang, N.; Yuan, L.; Wang, C.; Kan, J.; Xu, X. Deformation characteristics and stability analysis of roof roadway in destressed mining. *J. China Coal Soc.* **2011**, *36*, 1784–1789.
18. Kong, X.; Shan, R.; Ju, T. Model experiment of deformation and failure mechanism of coal roadway surrounding rock and its engineering application. *J. Min. Saf. Eng.* **2017**, *34*, 464–471.
19. Jaiswal, A.; Shrivastva, B.K. Numerical simulation of coal pillar strength. *Int. J. Rock Mech. Min. Sci.* **2009**, *46*, 779–788. [[CrossRef](#)]
20. Bertuzzi, R.; Douglas, K.; Mostyn, G. An Approach to model the strength of coal pillars. *Int. J. Rock Mech. Min. Sci.* **2016**, *89*, 165–175. [[CrossRef](#)]
21. Waclawik, P.; Ptacek, J.; Konicek, P.; Kukutsch, R.; Nemcik, J. Stress-state monitoring of coal pillars during room and pillar extraction. *J. Sustain. Min.* **2016**, *15*, 49–56. [[CrossRef](#)]
22. Gu, D.; Yan, Y.; Zhang, Y.; Wang, E.-Z. Experimental study and numerical simulation for dynamic response of coal pillars in coal mine underground reservoir. *J. China Coal Soc.* **2016**, *41*, 1589–1597.
23. Song, Y.; Yang, X. Evolution characteristics of deformation and energy fields during coal pillar instability. *J. Min. Saf. Eng.* **2013**, *30*, 822–827.
24. Zhang, J.; Wang, B. Stability of isolated coal pillar and overburden instability in shallow-buried interval gob. *J. Min. Saf. Eng.* **2020**, *37*, 936–942.
25. Zhang, C.; Han, P.; Wang, F.; He, X. The stability of residual coal pillar in underground reservoir with the effect of mining and water immersion. *J. China Coal Soc.* **2021**, *50*, 220–227.
26. Chen, D.; Wu, Y.; Xie, S.; He, F.; Sun, Y.; Shi, S.; Jiang, Z. Study on the first fracture of the main roof plate structure with one side goaf and elastic-plastic foundation boundary. *J. China Coal Soc.* **2021**, *46*, 3090–3105.
27. Zhao, H.; Cheng, H.; Wang, L.; Liu, Y.; Ji, D.; Zhang, Y. Distribution characteristics of deviatoric stress field and failure law of roadway surrounding rock under non-hydrostatic pressure. *J. China Coal Soc.* **2021**, *46*, 370–381.
28. Qi, X.; Deng, G.; Huang, K. Stress transfer law of coalpillar floor in room-pillar area of close distance coal seam. *J. Xi’an Univ. Sci. Technol.* **2021**, *41*, 649–656.
29. Tu, M.; Lin, Y.; Zhang, X.; Pu, Q.; Dang, J.; Zhao, G. Evolution of overburden structure and reasonable width of section coal pillar in large space isolated island stope. *J. Min. Saf. Eng.* **2021**, *38*, 857–865.
30. Wu, B. Reasonable Arrangement Mode About Coal Pillar Dam of Distributed Groundwater Reservoir in Coal Mine. *Saf. Coal Mines* **2018**, *49*, 68–72.
31. Cao, Z.; Ju, J.; Xu, J. Distribution model of water-conducted fracture main channel and its flow characteristics. *J. China Coal Soc.* **2019**, *44*, 3719–3728.
32. Xie, H.; Yao, Q.; Yu, L.; Shan, C. Study on damage characteristics of water-bearing coal samples under cyclic loading-unloading. *Sustainability* **2022**, *14*, 8457. [[CrossRef](#)]
33. Wu, B.; Wang, W.; Guo, D. Strength damage and AE characteristics of fractured sandstone under the influence of water intrusion times. *J. Min. Saf. Eng.* **2020**, *37*, 1054–1060.
34. Wang, F.; Liang, N.; Li, G.; Zhao, B. Failure evolution mechanism of coal pillar dams in complex stress environment. *J. Min. Saf. Eng.* **2019**, *36*, 1145–1152.

35. Wang, Z.; Ma, K.; Tian, H.; Li, Q. Numerical analysis of stress wave propagation law of coal and rock mass and its influencing factors. *Coal Sci. Technol.* **2019**, *47*, 66–72.
36. Guy, R.; Kent, M.; Russell, F. An assessment of coal pillar system stability criteria based on a mechanistic evaluation of the interaction between coal pillars and the overburden. *Int. J. Min. Sci. Technol.* **2017**, *27*, 11–17.
37. Yilmaz, I. Influence of water content on the strength and deformability of gypsum. *Int. J. Rock Mech. Min. Sci.* **2009**, *47*, 342–347. [[CrossRef](#)]
38. Verstrynge, E.; Adriaens, R.; Elsen, J.; Van Balen, K. Multi-scale analysis on the influence of moisture on the mechanical behavior of ferruginous sandstone. *Constr. Build. Mater.* **2014**, *54*, 78–90. [[CrossRef](#)]
39. Özdemir, E.; Sarici, D.E. Combined Effect of Loading Rate and Water Content on Mechanical Behavior of Natural Stones. *J. Min. Sci.* **2018**, *54*, 931–937. [[CrossRef](#)]
40. Du, J.; Meng, X. *Mining Science*; University of Mining and Technology Press: Beijing, China, 2009; pp. 389–393.
41. Qian, M.; Shi, P. *Mining Pressure and Strata Control*; China University of Mining and Technology Press: Beijing, China, 2003; pp. 108–109.
42. Zhang, Y.; Xu, L.; Liu, K. Formation mechanism and evolution laws of gas flow channel in mining coal and rock. *J. China Coal Soc.* **2012**, *37*, 1444–1446.
43. Zhou, X.; Zhang, Y. *Beijing: Constitutive Theory and Application of Unloading Rock Mass [M]*; Science Press: Beijing, China, 2007; pp. 55–72.
44. Chen, W. *Analysis Theory and Engineering Applications of Fissured Rock Mass Stability in Underground Engineering*; Science Press: Beijing, China, 2007; pp. 233–234.
45. Yang, J.; Hu, J.; Wu, Y.; Zhang, B. Numerical simulation of seepage and stability of tailing dams: A case study in ledong, China. *Sustainability* **2022**, *14*, 12393. [[CrossRef](#)]

Disclaimer/Publisher’s Note: The statements, opinions and data contained in all publications are solely those of the individual author(s) and contributor(s) and not of MDPI and/or the editor(s). MDPI and/or the editor(s) disclaim responsibility for any injury to people or property resulting from any ideas, methods, instructions or products referred to in the content.